Convective Fluid Flow and Heat Transfer in a Vertical Rectangular Duct Containing a Horizontal Porous Medium and Fluid Layer

J.C. Umavathi[1*] and O. Anwar Bég[2]

[1] *Professor of Applied Mathematics, Department of Mathematics, Gulbarga University, Gulbarga-585 106, Karnataka, **India.***
Email: *drumavathi@rediffmail.com*
[2] *Professor of Engineering Science & Director- Multi-Physical Engineering Sciences Group, Mechanical Engineering*

*Department, School of Science, Engineering and Environment (SEE), University of Salford, Manchester, M54WT, **UK.***

Email: O.A.Beg@salford.ac.uk / gortoab@gmail.com

*Corresponding author

Abstract

Purpose-A numerical analysis is presented to investigate thermally and hydrodynamically fully developed convection in a duct of rectangular cross-section containing a porous medium and fluid layer.

Design/methodology/approach-The Darcy-Brinkman-Forchheimer flow model is adopted. A finite difference method of second-order accuracy with the Southwell-Over-Relaxation Method (SORM) is deployed to solve the non-dimensional momentum and energy conservation equations under physically robust boundary conditions.

Findings-It is found that the presence of porous structure, and different immiscible fluids exert a significant impact in controlling the flow. Graphical results for the influence of the governing parameters i.e. Grashof number, Darcy number, porous media inertia parameter, Brinkman number and ratios of viscosities, thermal expansion and thermal conductivity parameters on the velocity and temperature fields are presented. The volumetric flow rate, skin friction and rate of heat transfer at the left and right walls of the duct are also provided in tabular form. The numerical solutions obtained are validated with the published work and excellent agreement is attained.

Originality/value-To the authors best knowledge this work original in developing the numerical code using FORTRAN to assess the fluid properties for immiscible fluids. The

study is relevant to geothermal energy systems, thermal insulation systems, resin flow modeling for liquid composite molding processes and hybrid solar collectors.

Keywords: *Mixed convection, finite difference, vertical duct, Darcy-Brinkman-Forchheimer model; interface; porous medium; Nusselt number.*

List of symbols

Roman symbols

$A^{(i)}$	aspect ratio in region-1 $\left(\dfrac{a^{(i)}}{2b}\right)$
$a^{(i)}$	height of the duct
b	width of the duct
C_F	porous media inertial coefficient
C_p	isobaric specific heat
Da	Darcy number $\left(\dfrac{\kappa}{b^2}\right)$
Gr	Grashof number $\left(\dfrac{g\,\rho^{(1)2}\,\beta^{(1)}b^3\left(T^{(w2)}-T^{(w1)}\right)}{\mu^{(1)2}}\right)$
I	dimensionless inertial parameter $\left(\dfrac{C_F\,b}{\sqrt{\kappa}}\right)$
$K^{(i)}$	thermal conductivity
β	ratio of thermal expansion co-efficient $\left(\dfrac{\beta_t^{(2)}}{\beta_t^{(1)}}\right)$
$Nx^{(i)}, Ny$	number of grids
n	ratio of densities $\left(\dfrac{\rho^{(2)}}{\rho^{(1)}}\right)$
P	pressure

p dimensionless gradient of pressure $\left(\dfrac{b^2}{\mu^{(1)}\, \overline{W}^{(1)}} \dfrac{\partial P}{\partial Z} \right)$

$T^{(i)}$ temperature

$T^{(wi)}$ wall temperature

$\overline{W}^{(i)}$ average velocity

$W^{(i)}$ velocity

w dimensionless velocity

$x,\ y,\ z$ dimensionless spatial coordinates

$\Delta x^{(i)}$ and Δy step lengths in the x and y directions

$X^{(i)}, Y, Z$ dimensional space coordinates

Greek Symbols

λ viscosity ratio $\left(\dfrac{\mu^{(1)}}{\mu^{(2)}} \right)$

$\beta^{(i)}$ thermal expansion coefficient

β ratio of thermal expansion coefficients $\left(\dfrac{\beta_t^{(2)}}{\beta_t^{(1)}} \right)$

κ permeability of the porous medium

χ conductivity ratio $\left(\dfrac{K^{(2)}}{K^{(1)}} \right)$

$\mu^{(i)}$ dynamic viscosity

θ dimensionless temperature

σ porous parameter $\left(\dfrac{b}{\sqrt{\kappa}} \right)$

ρ density of the fluid

ν kinematic viscosity of the fluid

Superscripts

$i = 1, 2$ quantities for region-1 and region-2 respectively.

Subscripts

1, 2   quantities for region-1 and 2, respectively.

1. Introduction

A vast amount of work, both theoretical and experimental, exists in the literature relating to thermal buoyancy effects in ducts. Important monographs in this regard include the books by Lewis *et al*. (2004) and Nitiarasu *et al.* (2016) which rigorously address the fundamentals of the finite element method for heat and mass transfer technological applications. This includes both *purely fluid* and *porous media systems*. Representative works on porous media in vertical enclosures include Prasad and Kulacki (1984), Beckermann *et al.* (1986) and Manole and Lage (1992) all of whom have studied diverse aspects of such flows. Convection in a homogeneous porous matrix enclosed in an oblique cavity was scrutinized numerically by Baytas and Pop (1999). Management of geothermal systems, heat pipes, phase change applications and transpiration cooling, resin mold fabrication, drying, biochemical filtration, storing and transporting energy are several important applications in industry where porous media are featured. Tien and Vafai (1989) and Amiri and Vafai (1995) pointed out that in a heat sink medium, porous insertions play a beneficial role in heat transfer. If the boundaries are impermeable then the classical Darcy law (valid for viscous-dominated low Reynolds number flows) however cannot be applied. In such cases the inclusion of inertia and boundary effects should be implemented. Engineers have therefore developed the Brinkman-Forchheimer-extended Darcy model which is a nonlinear drag force which has been shown to more accurately address these effects. The numerical approach for the porous channel using the Brinkman-Forchheimer-extended Darcy model was developed and applied extensively by Kaviany (1985), Vafai and Kim (1989) and Amiri and Vafai (1994). The finite element method in both static and dynamic consolidation of porous media with relevance to engineering geomechanics (including thermal transport) was lucidly elaborated in the excellent text by Lewis and Schrefler (1998). Nield and Bejan (1999),

Kaviany (1991) and Vafai (2000) further elaborated on porous media hydrodynamics and heat transfer with modified Darcy formulations. Umavathi and co-workers (2012a, 2012b, 2013, 2015a, 2015b) have subsequently rigorously researched many aspects of transport phenomena in fluid-saturated porous media in channels/ducts. Using the approach of the continuum theory of porous media (TPM) and particle-based Lattice Boltzmann method (LBM), Mohamad *et al.* (2020) provided detailed computational simulations of flow through porous media. These works robustly demonstrated that, coupling the TPM and LBM theories generated accurate and reliable simulations of realistic transport phenomena in deformable porous media.

Transport in *composite fluid-porous layers* has also attracted significant attention in engineering sciences in recent years. Many interesting applications of such flows arise including post-accident cooling of nuclear reactors (Kuznetsov, 1999), convection in fibrous insulations (Bagchi and Kulacki, 2020), thermal duct technology (Min and Kim, 2005), groundwater contamination (Khalili *et al.,* 2003), chemical reactor packed beds (Jones and Persichetti, 1986) and geothermal energy (Le Louis *et al.*, 2018). Beckerman *et al.* (1987) presented one of the first studies of flow in composite fluid-porous media systems. They reported both numerical and experimental results for a rectangular chamber blocked with a mixture of a fluid layer and porous layer and identified that the convective pattern was significantly transformed in comparison with the chamber comprising only either a clear fluid or a porous bed. Arquis and Caltagirine (1987) and Du and Bilgen (1990) also considered a similar composition and produced analogous observations corroborating the results reported by Beckerman *et al.* (1987). Assuming the impermeable condition at the interface between the porous and fluid layers, Campos *et al.* (1990) computed the flow patterns in a rectangular conduit. Song and Viskanta (1994) also carried out a detailed theoretical and experimental review on convection in rectangular enclosures partially filled with anisotropic porous media. Srinivasan and Vafai (1994) scrutinized the linear encroachment of an immiscible fluid in a saturated porous bed. The flow between two plates packed with immiscible fluids was examined by Kapur and Shukla (1964). Analytical solutions were derived by Srinivas and Ramana Murthy (2016a, b) for immiscible fluids adopting couple stress and micropolar fluid rheological models. Magnetic effects were explored by Borrelli *et al.* (2017) in a vertical

conduit containing electrically conducting immiscible fluids. For both fully and partially filled spheres in a cubic packing cavity, Manu *et al*. (2020) investigated numerically thermal convection flows. They concluded that for large values of Rayleigh number (natural convection parameter) the Darcy-Forchheimer simulations under-predict the heat transfer.

As noted earlier, flows in composite systems i.e. containing both a porous bed and an adjacent fluid layer are of considerable theoretical and practical interest. Melting of ice in frozen soils which arises owing to the changes in the weather is a further interesting application of transport phenomena between a porous bed and clear fluid. Mathematical models of transport in composite porous-fluid media also arise in crude-oil production, castings, biomedical (multi-phase tissue dynamics), foam fabrication, Gas Assisted Injection Molding (GAIM) and geophysical systems (Valette et al., 2004, Howell et al., 2000, Christian et al., 2006, Renger et at al., 2007, Cole et al., 2010). Much of the motivation for the current study stems from common multi-fluid flow operations present in the construction and completion of oil and gas wells, e.g., primary cementing, drilling, and hydraulic fracturing, and also geothermal reservoirs.

Umavathi and co-workers (Malashetty et al., 2001, 2004, 2005, Umavathi et al., 2004, 2005, 2008, 2010, 2012, 2014, 2019) conducted extensive investigations into the dynamics of immiscible flow in conduits considering steady, unsteady, Newtonian and non-Newtonian fluids scenarios. Prasad (1990) presented a succinct review of composite porous layer fluid dynamics. Simulation of composite porous medium flows has received considerable attention and was the focus of several investigations (Chikh et al. 1995, and Kim and Choi, 1996). The first attempt to robustly represent the conditions at the interface of fluid-porous media was made by Beavers and Joseph (1967). They identified the velocity slip at the interface by performing careful experiments. Neale and Nader (1974) later formulated the slip velocity boundary conditions at the interface for a porous medium. They introduced the Brinkman term in the momentum conservation equation for the porous zone and proposed the continuity of velocity and also the velocity gradient at the interface. Furthermore, an exact solution for composite porous media incorporating the inertial effects was determined by Vafai and Kim (1990). The continuity of velocity and the continuity of shear stress at the interface between the clear viscous fluid and

porous medium was considered in the study of Vafai and Kim (1990). Later, the flow of three immiscible fluids was analysed by Vafai and Thiyagaraja (1987) assuming continuity of shear stress and heat flux at the two interfaces, for the case in which clear fluid was sandwiched between porous media. Later Alzami and Vafai (2001) presented various types of interfacial conditions between a clear fluid and a porous medium, following the interface conditions proposed by Vafai and Thiyaaraja (1987).

The works in the literate on immiscible fluids is limited owing to the complex nature which arises at the interface and also due to the wetting/non-wetting characteristics when the fluid adheres to the solid boundary. Experimental (Hulin *et al.,* 2008) and computational (Sahu and Vanka, 2011, Redapangu *et al.,* 2012) works are available on buoyancy induced immiscible fluid flows which leave certain aspects unresolved and demand further elucidation. Motivated by this, we aim to introduce, for the first time, an immiscible two-dimensional model paving the way for more complex experimental and theoretical analyses to come in the future. The current study therefore addresses theoretically and numerically the buoyancy-induced flow in a vertical rectangular duct which is filled with both immiscible clear viscous fluid and viscous fluid saturated with a porous medium. The computations are relevant to mechanical engineering processes involving heat and mass transfer, chemical engineering packed beds, reservoir engineering thermal recovery processes, geothermic, fiber insulation, and also the dynamics of salty hot springs in ocean environments.

2. Governing Equations

The physical system (**Figure.1**) considered consists of a two-dimensional rectangular vertical duct filled with homogeneous isotropic porous and fluid layers. The Darcy-Brinkman-Forchheimer model is used, taking into account the effect of viscous and Darcy dissipations.
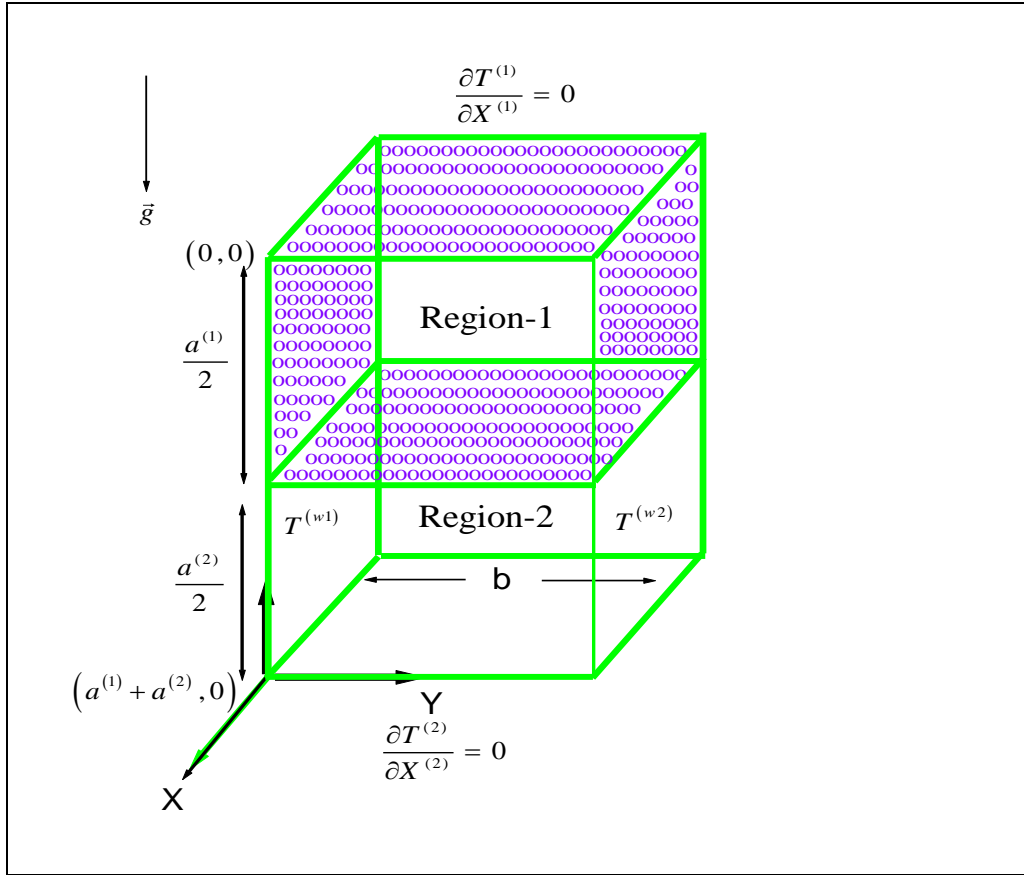
Figure 1. Schematic diagram

The flow is assumed to be fully developed, incompressible, steady and laminar. For fully developed flow the relations on U and V are $U = V = 0, \frac{\partial U}{\partial X} = \frac{\partial U}{\partial Y} = \frac{\partial V}{\partial X} = \frac{\partial V}{\partial Y} = 0$. By the equation of continuity one obtains $\frac{\partial W}{\partial Z} = 0$ and hence the velocity W along the Z direction of the fluid is non-vanishing. The length of the conduit is $\frac{(a_1 + a_2)}{2}$ and width is b. The region-1 $\left(0 \le X^{(1)} \le \frac{a^{(1)}}{2}, \, 0 \le Y \le b\right)$ is filled with a porous material having permeability κ. This region is saturated with a viscous fluid having density $\rho^{(1)}$, viscosity $\mu^{(1)}$, thermal expansion coefficient $\beta^{(1)}$ and thermal conductivity $K^{(1)}$. The region-2 $\left(\frac{a^{(1)}}{2} \le X^{(2)} \le \frac{a^{(2)}}{2}, \, 0 \le Y \le b\right)$ is filled with a different (immiscible) fluid

having density $\rho^{(2)}$, viscosity $\mu^{(2)}$, thermal expansion coefficient $\beta^{(2)}$ and thermal conductivity $K^{(2)}$. The top and bottom duct boundaries are insulated $\left(\dfrac{\partial T}{\partial X} = 0 \right)$, the left wall has constant temperature $T^{(w1)}$ and the right wall is at constant temperature $T^{(w2)}$ with the condition imposed as $T^{(w2)} > T^{(w1)}$ (i.e., heating at the right wall and cooling at the left wall). The fluids occupying the two regions are pure viscous fluid and possess constant physical properties except the density occurring in the buoyancy term (i.e. the Boussinesq approximation is taken into consideration). Mathematically the problem involves the coupling of the governing equations for the fluid region with the equations for the porous region through an appropriate set of *matching conditions* at the fluid/porous medium interface. We assume the continuity of velocity, shear stress, temperature and heat flux at the interface (Neale and Nader, 1974). As a first approximation we take μ_{eff} equal to the fluid viscosity μ_1 in the porous region. Also, a key assumption which is often adopted in the published literature is the thermal equilibrium between fluid in pores and solid material of the porous medium. For instance, Sozen and Kuzay (1996) have studied heat transfer in a tube enhanced with mesh screens by making use of the thermal equilibrium approximation. Kim *et al.* (1994) have studied heat transfer in a channel filled with porous material subjected to oscillatory flow with the non-Darcy approach but with the equilibrium assumption for thermal fields. Following these references, it is assumed that the fluid within the porous medium saturates the solid matrix and both are in local thermodynamic equilibrium. Under these assumptions, the governing equations of motion and energy under the Oberbeck-Boussinesq approximation reduce to (Nield and Bejan, 1999):

Region-1

$$\mu^{(1)} \frac{\partial^2 W^{(1)}}{\partial X^{(1)2}} + \mu^{(1)} \frac{\partial^2 W^{(1)}}{\partial Y^2} + \rho^{(1)} \vec{g} \, \beta^{(1)} \left(T^{(1)} - T_0 \right) - \frac{\mu^{(1)}}{\kappa} W^{(1)} - \frac{\rho^{(1)} C_F}{\sqrt{\kappa}} W^{(1)2} = \frac{\partial P}{\partial Z} \qquad (1)$$

$$\frac{\partial^2 T^{(1)}}{\partial X^{(1)2}} + \frac{\partial^2 T^{(1)}}{\partial Y^2} + \frac{\mu^{(1)}}{K^{(1)}} \left[\left(\frac{\partial W^{(1)}}{\partial X^{(1)}} \right)^2 + \left(\frac{\partial W^{(1)}}{\partial Y} \right)^2 \right] + \frac{\mu^{(1)}}{K^{(1)} \kappa} W^{(1)2} = 0 \qquad (2)$$

Region-2

$$\mu^{(2)}\,\frac{\partial^2 W^{(2)}}{\partial X^{(2)2}} + \mu^{(2)}\,\frac{\partial^2 W^{(2)}}{\partial Y^2} + \rho^{(2)}\,\vec{g}\,\beta^{(2)}\left(T^{(2)} - T_0\right) = \frac{\partial P}{\partial Z} \tag{3}$$

$$\frac{\partial^2 T^{(2)}}{\partial X^{(2)2}} + \frac{\partial^2 T^{(2)}}{\partial Y^2} + \frac{\mu^{(2)}}{K^{(2)}}\left[\left(\frac{\partial W^{(2)}}{\partial X^{(2)}}\right)^2 + \left(\frac{\partial W^{(2)}}{\partial Y}\right)^2\right] = 0 \tag{4}$$

The reference temperature is considered as $T_0 = \dfrac{\left(T^{(w1)} + T^{(w2)}\right)}{2}$. The flow is caused due to the pressure and temperature gradients. The velocity is zero (no-slip condition) at the boundaries. Following Alzami and Vafai (2001), it is assumed that there is continuity of velocity, temperature, shear stress and heat flux at the interface. In this direction, Equations (1) to (4) are solved subject to the following boundary and interface conditions:

$$W^{(1)} = 0, \qquad T^{(1)} = T^{w1} \qquad\qquad \text{at}\quad Y = 0 \quad\text{for}\ 0 \le X^{(1)} < \frac{a^{(1)}}{2}$$

$$W^{(1)} = 0, \qquad T^{(1)} = T^{w2} \qquad\qquad \text{at}\quad Y = b \quad\text{for}\ 0 \le X^{(1)} < \frac{a^{(1)}}{2}$$

$$W^{(1)} = 0, \qquad \frac{\partial T^{(1)}}{\partial X^{(1)}} = 0 \qquad\qquad \text{at}\quad X^{(1)} = 0 \quad\text{for}\ 0 \le Y \le b$$

$$W^{(1)} = W^{(2)}, \qquad \mu^{(1)}\frac{\partial W^{(1)}}{\partial X^{(1)}} = \mu^{(2)}\frac{\partial W^{(2)}}{\partial X^{(2)}} \qquad \text{at}\quad X = \frac{a^{(1)}}{2} \quad\text{for}\ 0 \le Y \le b$$

$$T^{(1)} = T^{(2)}, \qquad K^{(1)}\frac{\partial T^{(1)}}{\partial X^{(1)}} = K^{(2)}\frac{\partial T^{(2)}}{\partial X^{(2)}} \qquad \text{at}\quad X = \frac{a^{(1)}}{2} \quad\text{for}\ 0 \le Y \le b$$

$$W^{(2)} = 0, \qquad T^{(2)} = T^{w1} \qquad\qquad \text{at}\quad Y = 0 \quad\text{for}\ \frac{a^{(1)}}{2} < X^{(2)} \le \frac{a^{(2)}}{2}$$

$$W^{(2)} = 0, \qquad T^{(2)} = T^{w2} \qquad\qquad \text{at}\quad Y = 0 \quad\text{for}\ \frac{a^{(1)}}{2} < X^{(2)} \le \frac{a^{(2)}}{2}$$

$$W^{(2)} = 0, \qquad \frac{\partial T^{(2)}}{\partial X^{(2)}} = 0 \qquad\qquad \text{at}\quad X^{(2)} = \frac{a^{(1)} + a^{(2)}}{2} \quad\text{for}\ 0 \le Y \le b \tag{5}$$

Using the following dimensionless variables

$$x^{(1)} = \frac{X^{(1)}}{b}, \quad x^{(2)} = \frac{X^{(1)}}{b}, \quad y = \frac{Y}{b}, \quad w^{(1)} = \frac{\rho_1 b}{\mu_1} W^{(1)}, \quad w^{(2)} = \frac{\rho_2 b}{\mu_2} W^{(2)},$$

$$\theta^{(1)} = \frac{T^{(1)} - T^{(0)}}{T^{(w2)} - T^{(w1)}}, \quad \theta^{(2)} = \frac{T^{(2)} - T^{(0)}}{T^{(w2)} - T^{(w1)}} \tag{6}$$

Equations (1) to (4) can be written as follows:

Region-1

$$\frac{\partial^2 w^{(1)}}{\partial x^{(1)2}} + \frac{\partial^2 w^{(1)}}{\partial y^2} + Gr\,\theta^{(1)} - \frac{1}{Da} w^{(1)} - I\,w^{(1)2} = p \tag{7}$$

$$\frac{\partial^2 \theta^{(1)}}{\partial x^{(1)2}} + \frac{\partial^2 \theta^{(1)}}{\partial y^2} + Br\left[\left(\frac{\partial w^{(1)}}{\partial x^{(1)}}\right)^2 + \left(\frac{\partial w^{(1)}}{\partial y}\right)^2\right] + \frac{Br}{Da} w^{(1)2} = 0 \tag{8}$$

Region-2

$$\frac{\partial^2 w^{(2)}}{\partial x^{(2)2}} + \frac{\partial^2 w^{(2)}}{\partial y^2} + \frac{Gr\,\beta\,n}{\lambda} \theta^{(2)} = \frac{p}{\lambda} \tag{9}$$

$$\frac{\partial^2 \theta^{(2)}}{\partial x^{(2)2}} + \frac{\partial^2 \theta^{(2)}}{\partial y^2} + \frac{Br\,\lambda}{K}\left[\left(\frac{\partial w^{(2)}}{\partial x^{(2)}}\right)^2 + \left(\frac{\partial w^{(2)}}{\partial y}\right)^2\right] = 0 \tag{10}$$

The boundary and interface conditions given in Equation (5) using Equation (6) become:

$$w^{(1)} = 0, \qquad \theta^{(1)} = -\frac{1}{2} \qquad \text{at} \quad Y = 0 \quad \text{for} \quad 0 \le x^{(1)} < A^{(1)}$$

$$w^{(1)} = 0, \qquad \theta^{(1)} = \frac{1}{2} \qquad \text{at} \quad Y = 1 \quad \text{for} \quad 0 \le x^{(1)} < A^{(1)}$$

$$w^{(1)} = 0, \qquad \frac{\partial \theta^{(1)}}{\partial x^{(1)}} = 0 \qquad \text{at} \quad x^{(1)} = 0 \quad \text{for} \quad 0 \le y \le 1$$

$$w^{(1)} = w^{(2)}, \qquad \frac{\partial w^{(1)}}{\partial x^{(1)}} = \frac{1}{\alpha}\frac{\partial w^{(2)}}{\partial x^{(2)}} \qquad \text{at} \quad x = A^{(1)} \quad \text{for} \quad 0 \le y \le 1$$

$$\theta^{(1)} = \theta^{(2)}, \qquad \frac{\partial \theta^{(1)}}{\partial x^{(1)}} = \beta\frac{\partial \theta^{(2)}}{\partial x^{(2)}} \qquad \text{at} \quad x = A^{(1)} \quad \text{for} \quad 0 \le Y \le 1$$

$$w^{(2)} = 0, \qquad \theta^{(2)} = -\frac{1}{2} \qquad\qquad \text{at} \quad y = 0 \qquad \text{for} \quad A^{(1)} < x^{(2)} \leq A^{(2)}$$

$$w^{(2)} = 0, \qquad \theta^{(2)} = \frac{1}{2} \qquad\qquad \text{at} \quad y = 0 \qquad \text{for} \quad A^{(1)} < x^{(2)} \leq A^{(2)}$$

$$w^{(2)} = 0, \qquad \frac{\partial \theta^{(2)}}{\partial x} = 0 \qquad\qquad \text{at} \quad x = A^{(1)} + A^{(2)} \qquad \text{for} \quad 0 \leq y \leq 1 \qquad (11)$$

where Gr is the Grashof number, Da is the Darcy number, I is the Forchheimer inertial coefficient, Br is the Brinkman number, β is the ratio of thermal expansion coefficient, n is the ratio of densities, λ is the ratio of viscosities, χ is the ratio of thermal conductivities, A_1 is the aspect ratio of region-1 and A_2 is the aspect ratio of region-2 which are defined as follows:

$$Gr = \frac{g \, \rho^{(1)2} \, \beta^{(1)} b^3 \left(T^{(w2)} - T^{(w1)} \right)}{\mu^{(1)2}}, \quad Da = \frac{\kappa}{b^2}, \; I = \frac{C_F \, b}{\sqrt{\kappa}}, \quad p = \frac{b^2}{\mu^{(1)} \, \overline{w}^{(1)}} \frac{\partial P}{\partial Z}$$

$$Br = \frac{\mu^{(1)3}}{K^{(1)} \, \rho^{(1)2} \, b^2 \left(T^{(w2)} - T^{(w1)} \right)}, \; \beta = \frac{\beta^{(2)}}{\beta^{(1)}}, \quad n = \frac{\rho^{(2)}}{\rho^{(1)}}, \; \lambda = \frac{\mu^{(1)}}{\mu^{(2)}}, \; K = \frac{K^{(2)}}{K^{(1)}}, \qquad (12)$$

$$A^{(1)} = \frac{a^{(1)}}{2b}, \quad A^{(2)} = \frac{a^{(2)}}{2b}$$

3. Numerical solutions

The numerical solutions of the governing equations are performed by the finite difference method (FDM). The discretization is achieved on finite mesh. The convection-diffusion terms are discretized using Taylor expansions, replacing the first and second order derivatives through first and second order central finite differencing approximations. The pressure gradient is assumed to be constant. The grid distribution is uniform and the grids chosen are $i = 1$ to $Nx1$ in region-1 $\left(x_i^{(1)}, y_j \right)$, $i = 1$ to $Nx2$ in region-2 $\left(x_i^{(2)}, y_j \right)$, and $j = 1$ to Ny in both regions. Δx is taken as the step length in $x-$direction and Δy is taken as the step length in y-direction (for details refer to Umavathi and Bég, 2020). Adopting the above procedure, the nonlinear, coupled partial differential equations as defined in Equations (7) to (10) along with corresponding

boundary and interface conditions as chosen from Equation (11) assume the following finite difference formations.

Region-1

$$\left(\frac{w^{(1)}_{i+1,j} - 2w^{(1)}_{i,j} + w^{(1)}_{i-1,j}}{\left(\Delta x^{(1)}\right)^2}\right) + \left(\frac{w^{(1)}_{i,j+1} - 2w^{(1)}_{i,j} + w^{(1)}_{i,j-1}}{\left(\Delta y\right)^2}\right) + Gr\,\theta^{(1)}_{i,j} - \tag{13}$$

$$\frac{1}{Da}w^{(1)}_{i,j} - I\,w^{(1)2}_{i,j} - p = 0$$

$$\left(\frac{\theta^{(1)}_{i+1,j} - 2\theta^{(1)}_{i,j} + \theta^{(1)}_{i-1,j}}{\left(\Delta x^{(1)}\right)^2}\right) + \left(\frac{\theta^{(1)}_{i,j+1} - 2\theta^{(1)}_{i,j} + \theta^{(1)}_{i,j-1}}{\left(\Delta y\right)^2}\right) + \tag{14}$$

$$Br\left[\left(\frac{w^{(1)}_{i+1,j} - w^{(1)}_{i-1,j}}{2\Delta x^{(1)}}\right)^2 + \left(\frac{w^{(1)}_{i,j+1} - w^{(1)}_{i,j-1}}{2\Delta y}\right)^2\right] + \frac{Br}{Da}w^{(1)2}_{i,j} = 0$$

Region-2

$$\left(\frac{w^{(2)}_{i+1,j} - 2w^{(2)}_{i,j} + w^{(2)}_{i-1,j}}{\left(\Delta x^{(2)}\right)^2}\right) + \left(\frac{w^{(2)}_{i,j+1} - 2w^{(2)}_{i,j} + w^{(2)}_{i,j-1}}{\left(\Delta y\right)^2}\right) + \frac{Gr\,\beta n}{\lambda}\theta^{(2)}_{i,j} - \frac{p^{(1)}}{\lambda} = 0 \tag{15}$$

$$\left(\frac{\theta^{(2)}_{i+1,j} - 2\theta^{(2)}_{i,j} + \theta^{(2)}_{i-1,j}}{\left(\Delta x^{(2)}\right)^2}\right) + \left(\frac{\theta^{(2)}_{i,j+1} - 2\theta^{(2)}_{i,j} + \theta^{(2)}_{i,j-1}}{\left(\Delta y\right)^2}\right) + \tag{16}$$

$$\frac{Br\,\lambda}{K}\left[\left(\frac{w^{(2)}_{i+1,j} - w^{(2)}_{i-1,j}}{2\Delta x^{(2)}}\right)^2 + \left(\frac{w^{(2)}_{i,j+1} - w^{(2)}_{i,j-1}}{2\Delta y}\right)^2\right] = 0$$

The associated boundary conditions are:

$$w^{(1)}_{i,0} = -w^{(1)}_{i,1}, \qquad \theta^{(1)}_{i,0} = -1 - \theta^{(1)}_{i,1}, \qquad\qquad \text{at}\quad Y = 0 \quad \text{for}\ 0 \le x^{(1)} < A^{(1)}$$

$$w^{(1)}_{i,Ny+1} = -w^{(1)}_{i,Ny}, \qquad \theta^{(1)}_{i,Ny+1} = 1 - \theta^{(1)}_{i,Ny} \qquad\qquad \text{at}\quad Y = 1 \quad \text{for}\ 0 \le x^{(1)} < A^{(1)}$$

$$w^{(1)}_{0,j} = -w^{(1)}_{1,j}, \qquad \theta^{(1)}_{1,j} = \theta^{(1)}_{0,j} \qquad\qquad\qquad \text{at}\quad x^{(1)} = 0 \quad \text{for}\ 0 \le y \le 1$$

$$\left.\begin{aligned} w^{(2)}_{Nx2+1,j} &= w^{(1)}_{Nx+1,j} + w^{(1)}_{Nx1,j} - w^{(2)}_{Nx2,j}\,, \\[2mm] w^{(1)}_{Nx+1,j} &= \frac{\Delta x^{(1)}}{\alpha\,\Delta x^{(2)}}\left(w^{(2)}_{Nx2,j} - w^{(2)}_{Nx2+1,j}\right) + w^{(1)}_{Nx1,j}, \end{aligned}\right\} \quad \text{at}\ x = A^{(1)} \quad \text{for}\ 0 \le y \le 1$$

$$\theta^{(2)}{}_{Nx2+1,j} = \theta^{(1)}{}_{Nx+1,j} + \theta^{(1)}{}_{Nx1,j} - \theta^{(2)}{}_{Nx2,j} \; ,$$

$$\theta^{(1)}{}_{Nx+1,j} = \beta \frac{\Delta x^{(1)}}{\Delta x^{(2)}}\left(\theta^{(2)}{}_{Nx2,j} - \theta^{(2)}{}_{Nx2+1,j}\right) + \theta^{(1)}{}_{Nx1,j},$$

$$\left.\right\} \quad \text{at } x = A^{(1)} \quad \text{for } 0 \leq Y \leq 1$$

$$w^{(2)}{}_{i,0} = -w^{(2)}{}_{i,1}, \quad \theta^{(2)}{}_{i,0} = -1 - \theta^{(2)}{}_{i,1}, \qquad\qquad \text{at } \quad y=0 \quad \text{for } A^{(1)} < x^{(2)} \leq A^{(2)}$$

$$w^{(2)}{}_{i,Ny+1} = -w^{(2)}{}_{i,Ny}, \qquad\qquad \theta^{(2)}{}_{i,Ny+1} = 1 - \theta^{(2)}{}_{i,Ny} \qquad\qquad \text{at } \quad y=0 \quad \text{for } A^{(1)} < x^{(2)} \leq A^{(2)}$$

$$w^{(2)}{}_{0,j} = -w^{(2)}{}_{1,j}, \qquad\qquad \theta^{(2)}{}_{1,j} = \theta^{(2)}{}_{0,j} \qquad\qquad \text{at } \quad x = A^{(1)} + A^{(2)} \quad \text{for } 0 \leq y \leq 1$$

$$(17)$$

The difference equations as given in Equations (12) to (16) along with boundary and interface conditions as given in Equation (17) are iterated incorporating the Southwell-Over-Relaxation method (ORM). The iteration is carried out until the tolerance value is achieved. The tolerance value is fixed as 10^{-8}. The validation of the code is carried out in two ways as follows:

1. **Grid independence study**: Table-1 provides the value of average Nusselt number at the left wall of the conduit for different sizes of grids. This table infers that the grid sizes 101x101 or 201x201 do not show any noticeable changes in the solutions. That is to say that the solutions obtained using 101x101 and 201x201 agree very well, hence choosing either 101x101 or 201x201 does not alter the flow structure i.e. grid independence is achieved. Hence the 101x101 grid size is adapted for the computations.

2. **Validation of the code with previous studies**: The results obtained in the present code are compared with Umavathi and Bég (2020) in the absence of porous material. The validation of the code in Umavathi and Bég (2020) is carried in detail by comparing with Oztop *et al.* (2009) for a composite system, Moshkin (2002) for a two-layer system in an enclosure and Davis (1963, 1983). Therefore, the present FDM solutions concur with Umavathi and Bég (2020) in the absence of a porous matrix for pure viscous immiscible fluids. Table-2 provides the values of average Nusselt number at the left plate for composite porous medium and viscous immiscible fluids (Umavathi and Bég, 2020). This table indicates that for large Grashof number, Nusselt number is less in Region-1 in comparison with Region-2. Further the Nusselt number for clear viscous fluid (Region-2) is close to Umavathi and Bég, (2020). One should note at this point that,

the Nusselt number for a composite porous medium in Region-2 (viscous fluid) will be different from the Nusselt number obtained for immiscible fluids owing to the contribution of the *interface dragging effect* for the porous matrix.

4. Results and discussion

The influence of interface conditions occurring between a fluid layer and a porous layer inside a vertical duct on the velocity and temperature distributions, is studied for various Grashof number (Gr), Darcy number (Da), inertial parameter (I), Brinkman number (Br), viscosity ratio (α), thermal expansion ratio (β) and thermal conductivity ratio (χ). The prescribed data values (unless otherwise stated) are $Gr = 10.0,\ Da = 0.01,\ I = 4.0,\ Br = 1.0,\ \lambda = 1.0,\ \beta = 1.0,\ \chi = 1.0,\ P = -1.0$ and the variations chosen are $0 \leq Gr \leq 10$, $0.00000 \leq Da \leq 1$, $0 \leq I \leq 8$, $0.1 \leq \lambda \leq 1$, $0.1 \leq \chi \leq 1$ - these values are selected from the literature (Pop and Ingham, 2001, Shail, 1973 and Vafai and Kim 1990).

The visualization of the distribution of velocity and temperature fields are presented via three-dimensional $(3D)$ and two-dimensional $(2D)$ contours and also profiles in one dimension $(1D)$. The purpose of considering the visualization in $3D$, $2D$ and $1D$ is to understand the distribution in a more elegant way. In plotting the one dimensional graphs, the y direction profiles varies from 0 to 1 at $x = 0.5$. The graphs portrayed in $3D$ appear at the top (denoted by the letter "a") followed by $2D$ (denoted by letter "b") contours.

Figures 2a and 2b illustrate the velocity and temperature contours for the effect of Grashof number. Gr is the ratio of buoyancy force to viscous force. Increasing the Grashof number indicates that the buoyancy forces dominates the viscous forces, which results in an enhancement of thermal convection. For $Gr = 0$, thermal buoyancy forces vanish and the flow is due to purely thermal conduction and since the right wall possesses a greater temperature in comparison with the left wall $\left(T^{(w1)} > T^{(w2)} \right)$, hence the $3D$ contour plot for $Gr = 0$ shows that the velocity is dominant at the right wall in comparison with the left wall. This can also be justified by noting that the number of

contours are dense at the right wall in comparison with the left wall as seen in the $2D$ graph. For $Gr = 1$, thermal buoyancy and viscous hydrodynamic forces are equal and the upward direction velocity is more in comparison with the downward direction $(3D)$, the number of contours are less in the lower region $(0 \leq y \leq 0.5)$ in comparison with the upper region $(0.5 \leq y \leq 1)$ $(2D)$. For $Gr = 0$, there is almost a symmetric distribution of velocity in the upward and downward directions $(3D)$ and the number of contours are equal in both the upper and lower regions $(2D)$. The figure 2b indicates that there is no significant influence of Gr on the temperature distribution for all values of Grashof number. The temperature distribution is almost linear and symmetric in both the upper and lower regions. The effect of Gr in Fig. 2c and 2d clearly illustrates that as Gr increases both the velocity and temperature increase i.e. momentum is assisted as is thermal diffusion. This is a classical result since as Gr increases, physically the intensification in thermal convection currents energizes the flow, as noted by Gebhart *et al*. (1988).

The enact of Darcy number on the velocity and temperature fields are displayed in **Figs**. 3a, b, c, d. As Da increases the velocity increases only in the lower region $(3D)$. Physically small values of Da implies the porous matrix is densely packed (the permeability is minute), therefore for $Da = 0.000001$, there is negligible velocity occurring in the region $0 \leq x \leq \dfrac{a^{(1)}}{2}$ ($2D$ graph shows no contours in this region). The velocity contours are symmetric for $Da = 0.01$, 1. However for $Da = 0.01$, the contours are flattened in comparison with $Da = 1$. Furthermore, the number of contours in the upper region (porous medium) are less in comparison with the lower region (clear viscous fluid). The impact of Darcy number does not induce any noticeable deviation and the contours are symmetric with respect to the horizontal symmetric line. The effective influence of Da is to increase the velocity and also the temperature i.e. to accelerate the flow and to heat the regime. The enhancement is however more prominent in velocity (Fig. 3c) in comparison with the temperature (Fig. 3d). The large Darcy

number implies a corresponding reduction in friction drag which results in the increase of velocity in the porous region in comparison with the clear viscous fluid region.

In **Figs. 4a, b, c** the velocity and temperature distributions for variation of inertial parameter (I) are depicted. The $3D$ graph reveals that the velocity is not significantly depleted with the inertial drag resistance in the upward and downward directions. However the shape of the contours in the $2D$ plot clearly shows that the contours are flat in region-1 (porous medium) in comparison with the contours in region-2 (clear viscous fluid). In Figs. 4b and 4c (when magnified) one can identify that the inertial drag generally reduces both the velocity and temperature fields i.e. it induces flow deceleration and cooling in the regime.

An increase in Brinkman number manifests in a noticeable increase in the velocity in both upward and downward directions (**Fig. 5a**). Figures 5b and 5c when magnified depict that both velocity and temperature distributions are boosted by enlarging the Brinkman number. Physically increase in the Brinkman number is associated with elevation in viscous dissipation effects which causes the increase in temperature and hence velocity is increased through the buoyancy term.

The effect of viscosity ratio $\left(\lambda = \dfrac{\mu^{(1)}}{\mu^{(2)}} \right)$ on the flow field is displayed in **Figs. 6a, b, c**. For values of $\lambda = 0.1$ $\left(\mu^{(2)} = 10 \ \mu^{(1)} \right)$ indicates that the saturated porous medium is ten times more viscous than the clear fluid, $\lambda = 0.5$ $\left(\mu^{(2)} = 2 \ \mu^{(1)} \right)$ implies that the fluid in region-1 is twice as viscous in comparison with the fluid in region-2, $\lambda = 1$ $\left(\mu^{(2)} = \mu^{(1)} \right)$ implies that the viscosity of the fluid in both regions are equal. In view of this for $\lambda = 0.1$, there is almost no flow in region-1, for $\lambda = 0.5$, the flow is slow in region-1 and for $\lambda = 1.0$, the flow is almost equivalent in both the regions. Figure 6a shows that the flow is accelerated in region-1 as λ increases $(3D)$; evidently in the $2D$ graphs there are *no velocity contours* in region-1 and *relatively few contours* for $\lambda = 0.5$ and *significantly more contours* for $\lambda = 1.0$. Figures 6b and 6c clearly reveal that as λ increases the velocity and temperature are both suppressed in region -1.

The effect of inertial parameter, Brinkman number and viscosity ratio on the temperature distributions exhibits a similar response for $3D$ and $2D$ to that of Grashof number and hence are excluded for brevity. The effect of thermal conductivity ratio $\left(\chi = \dfrac{K^{(2)}}{K^{(1)}}\right)$ is visualized in Figs. 7a, b, c, d. The $3D$ graphs do not precisely locate impact of χ, as the velocity contours resemble each other for all values of χ. Figure 7b depicts that the $2D$ temperature contours are weakly nonlinear for $\chi = 0.1$ in comparison with $\chi = 0.5, 1$. Figure 7c, d showcase that both the velocity and temperature decrease as χ increases. However, the effect of χ is not substantial on the velocity field. The impact of λ and χ are similar to the impact of these parameters described in an earlier study by Umavathi and Bég (2020). All the results are drawn considering equal height and width of the duct (square duct) i.e. the *aspect ratio is unity*.

The volumetric flow rate, skin friction and average Nusselt number at the left and right walls of the duct have also been computed and are provided in **Tables-3, 4, 5** respectively. The volumetric flow rate increases with higher Grashof number, Darcy number and Brinkman number whereas it decreases with increment in inertial parameter, viscosity ratio and conductivity ratio, in *both regions*. These trends are largely attributable to the accelerating influence of thermal buoyancy (Grashof number), porous medium permeability (Darcy number) and viscous dissipation effect (Brinkman number) and the retarding influence of inertial parameter (second order Forchheimer drag), viscosity ratio and conductivity ratio. The skin friction at the left wall, $\dfrac{dw}{dy}$ at $y = 0$ and at the right wall $\dfrac{dw}{dy}$ at $y = 1$ for both the regions are given in Table-4. The skin friction increases for large values of Grashof number, and Darcy number at both duct walls and in both regions. An upsurge in Brinkman number decreases the skin friction at the left wall and increases at the right wall for both regions and the converse behavior is induced (i.e. increasing skin friction at the left wall and reducing skin friction at the right wall) with an elevation in thermal conductivity ratio. An enhancement in the inertial (Forchheimer) parameter suppresses the skin friction at both the walls for region-1 and region-2 i.e.

consistently results in flow retardation at the duct boundaries. The average Nusselt number increases at the left wall and decreases at the right wall with greater magnitudes of Grashof number, Darcy number and Brinkman number for both duct regions. A rise in inertial parameter, viscosity ratio and conductivity ratio produce the reverse effect i.e. they consistently decrease the Nusselt number at the left wall and increase it at the right wall in both regions of the duct.

5. Conclusions

Motivated by applications in geothermics, thermal insulation and industrial energy systems, a mathematical model has been developed for the thermally developing convection flow through a duct of rectangular cross section occupied by composite porous medium i.e. a fluid layer and porous medium layer. Variable thermophysical properties have been considered and also viscous heating. The Darcy-Brinkman-Forchheimer formulation has been implemented. The governing conservation equations have been rendered non-dimensional with appropriate boundary conditions at the boundaries and the fluid/porous medium interface. A finite difference method along with Southwell's Successive Over Relaxation method has been applied to solve the transformed nonlinear boundary value problem with appropriate physical data, A grid (mesh) independence study has been conducted. Validation with earlier studies has also been included. Extensive visualization of results has been presented for the influence of the key governing parameters. The present simulations have shown that:

(i)Increasing Grashof, Darcy and Brinkman numbers promotes the velocity while elevation in inertial parameter, viscosity ratio and thermal conductivity ratio demotes the velocity.

(ii)The temperature is not significantly modified with any of the governing parameters except the thermal conductivity ratio.

(iii) The volumetric flow rate is considerably enhanced with higher values of Grashof, Darcy and Brinkman numbers whereas it is suppressed with greater values of the inertial (Forchheimer), viscosity ratio and conductivity ratio parameters.

(iv) Elevation in Grashof and Darcy numbers increases the skin friction at both walls for the two regions whereas a rise in Brinkman number (viscous dissipation) decreases the skin friction at the left wall and increases it at the right wall.

(v) For both the regions the average Nusselt number increases at the left wall and decreases at the right wall with a boost in Grashof, Darcy and Brinkman numbers. The opposite trend is computed with an elevation in the inertial parameter, viscosity ratio and conductivity ratio.

(vi) In the absence of porous matrix the results agree with those computed earlier in Umavathi and Bég (2020).

The present finite difference and SOR methodology is a versatile approach in immiscible and porous media thermofluid dynamic analysis. However, the model has assumed the porous medium to be rigid i.e. *non-deformable*. Future studies may consider deformability of the porous medium which is important in thermoelastic geological systems (boreholes, reservoir formations) and stratified flows and will be communicated in the near future.

(2a)
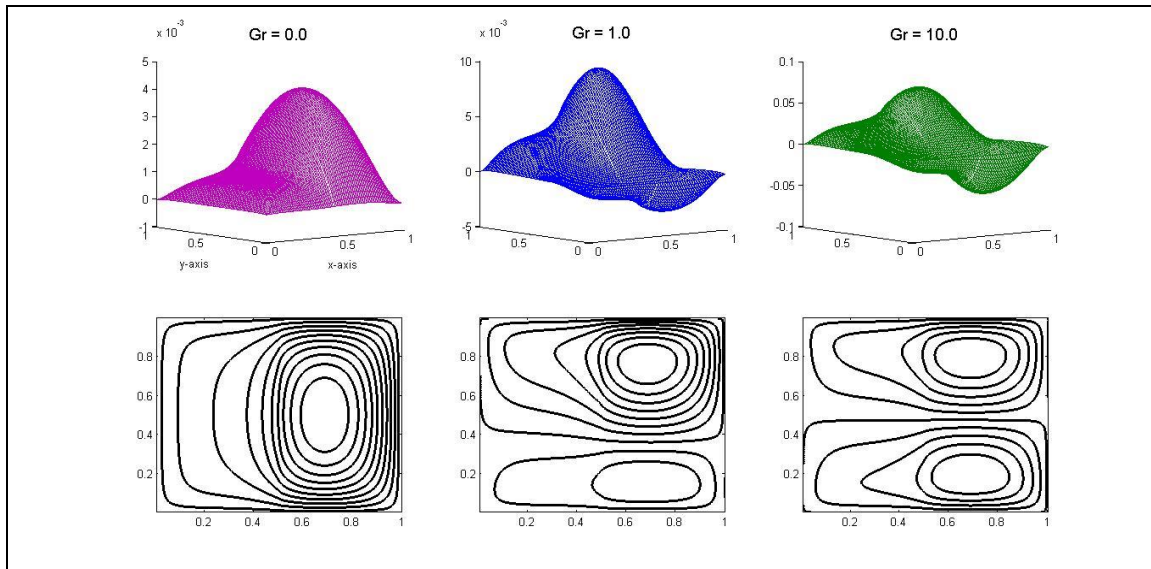
(2b)
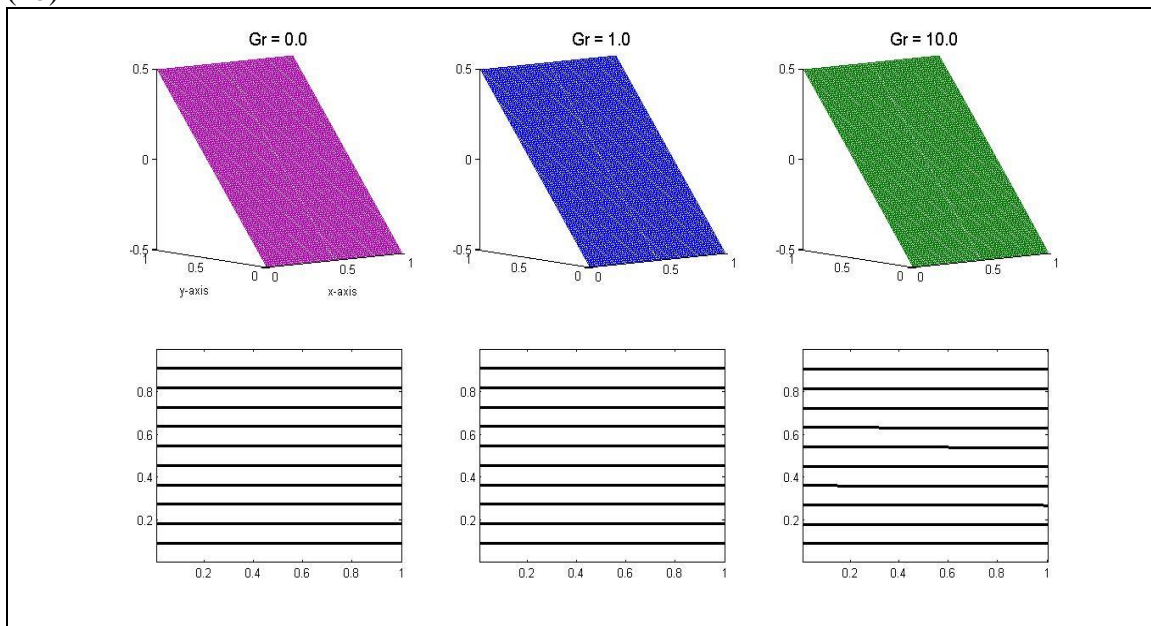
(2c)   (2d)
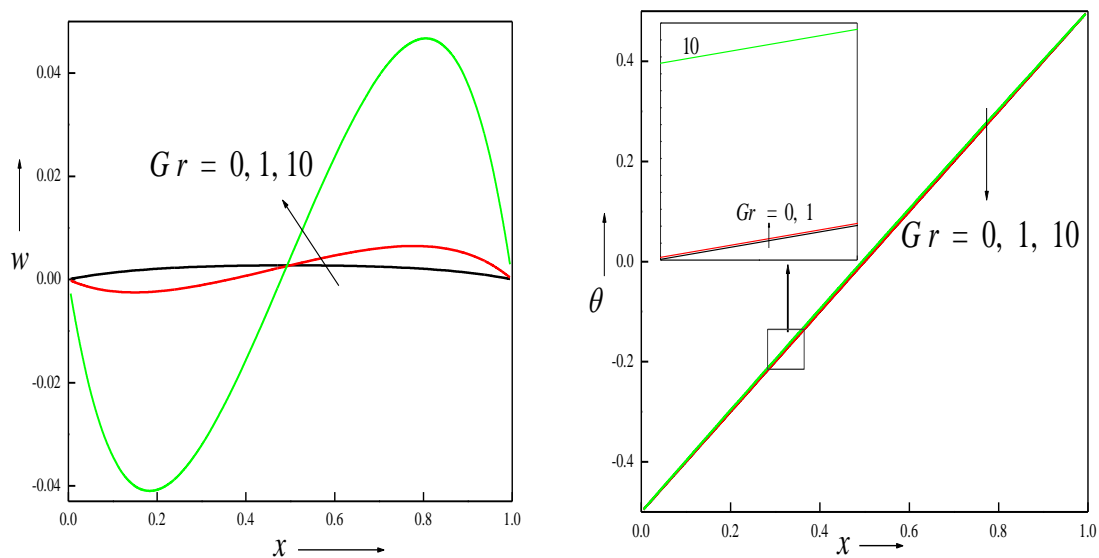
Figure 2. Velocity (2a, c) and temperature (2b, d) contours and profiles for different *Gr*

(3a)
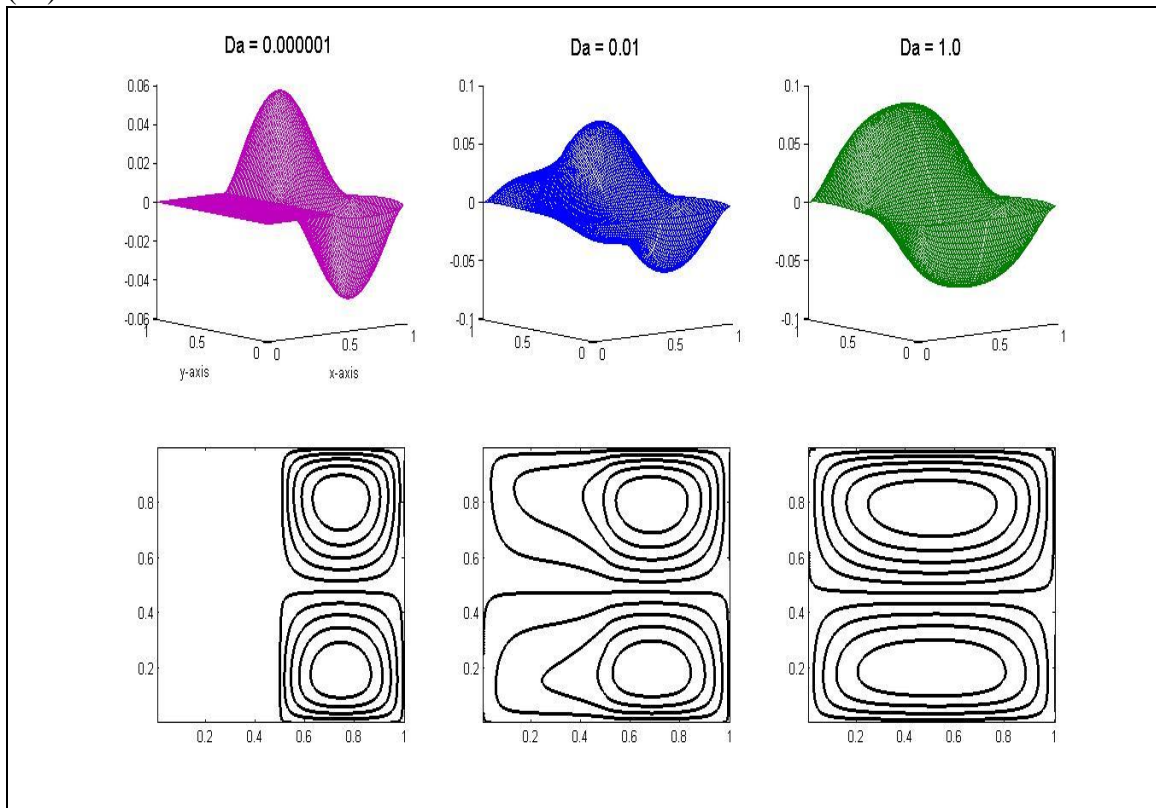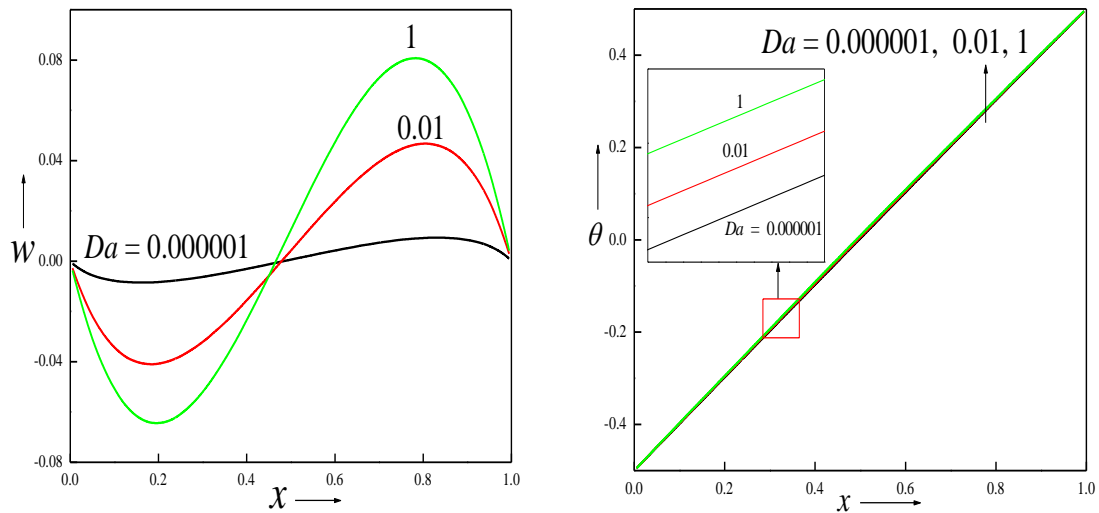

(3b)
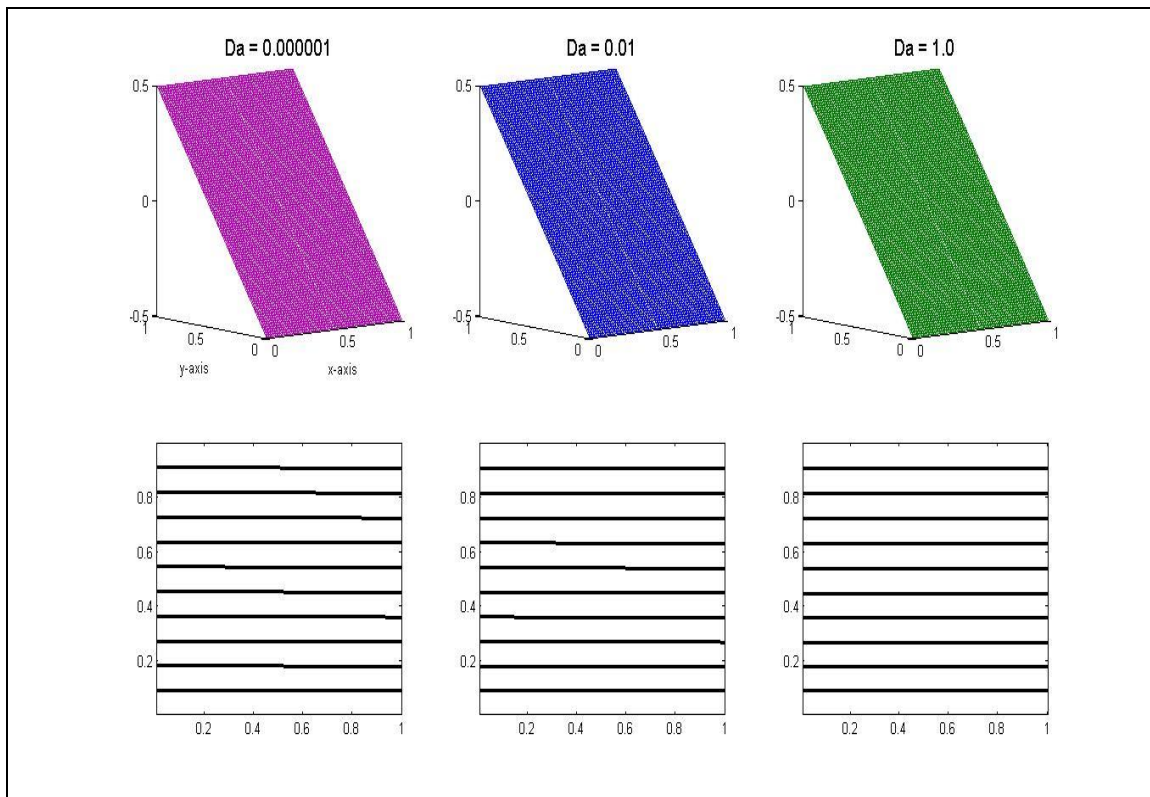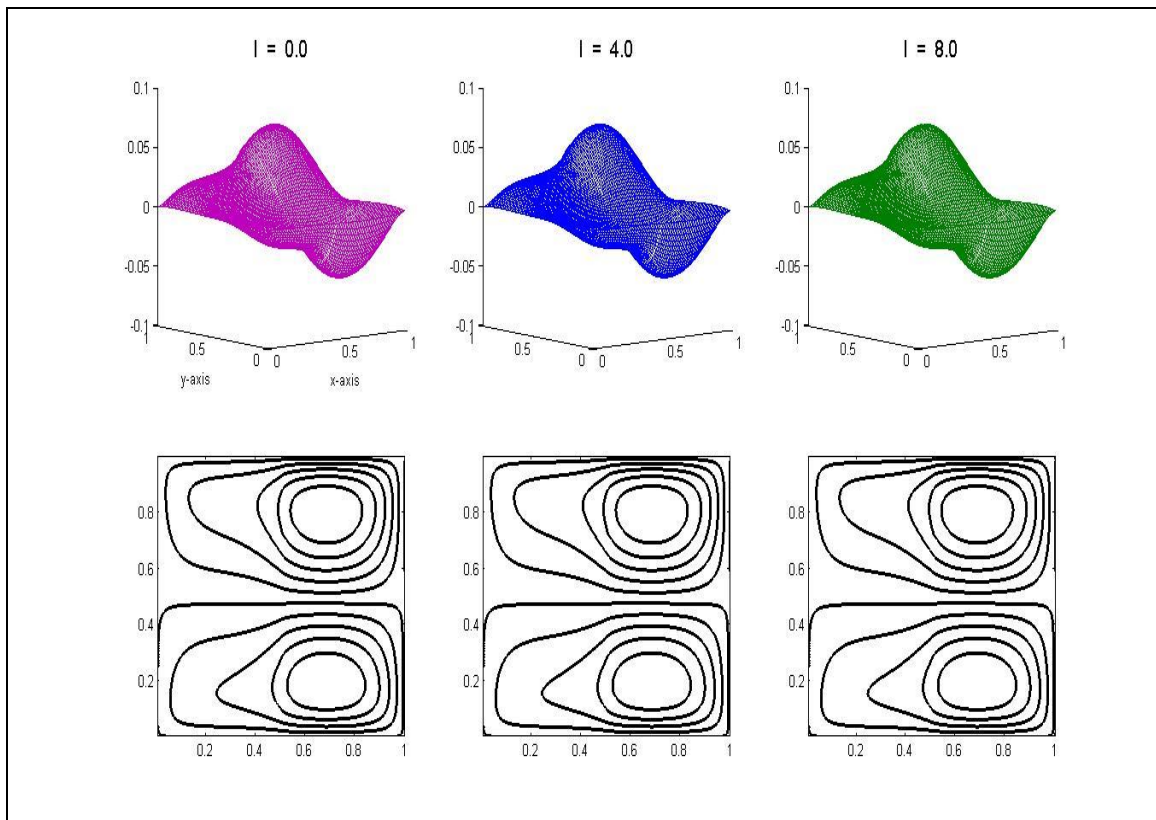
(3c)   (3d)
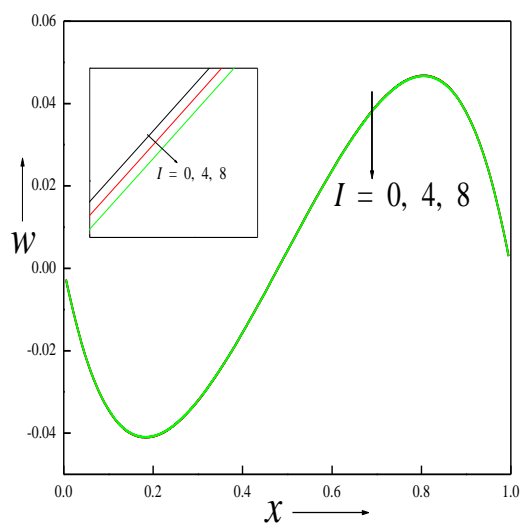

Figure 3. Velocity (3a, c) and temperature (3b, d) contours and profiles for different *Da*
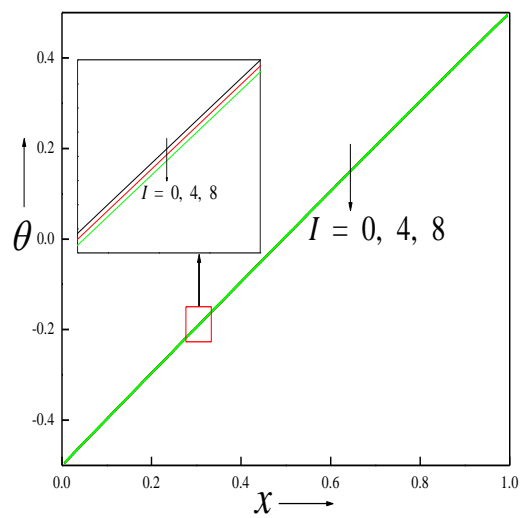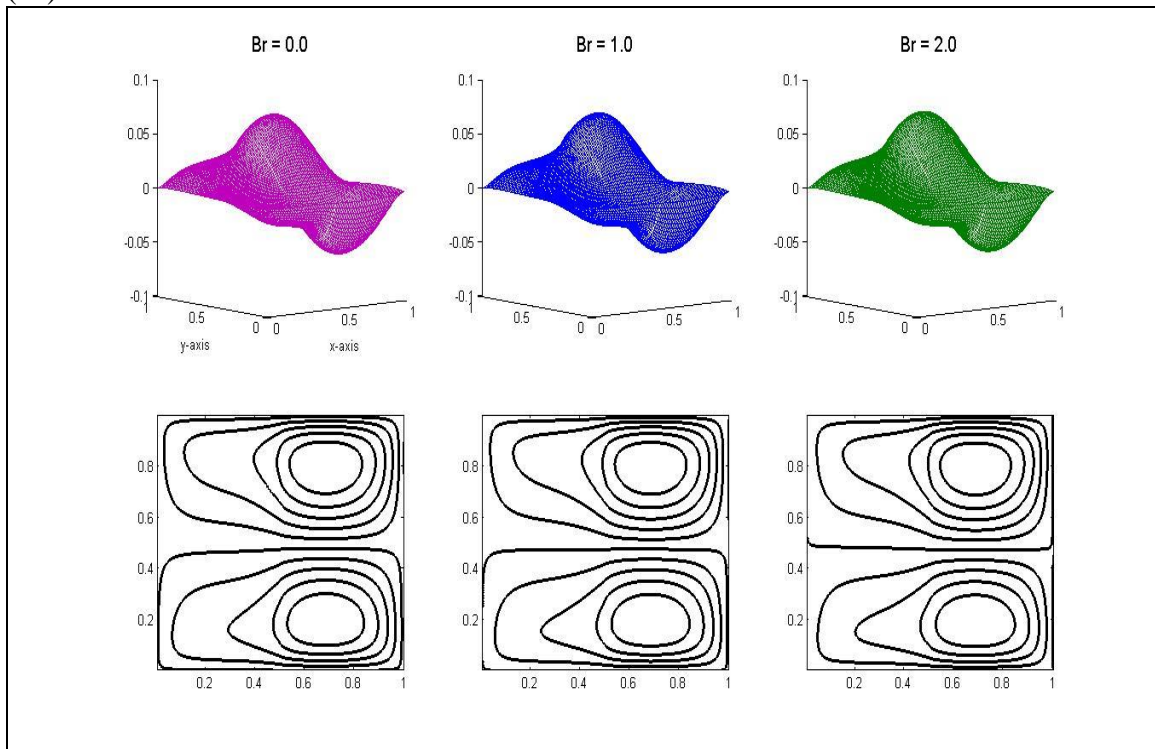
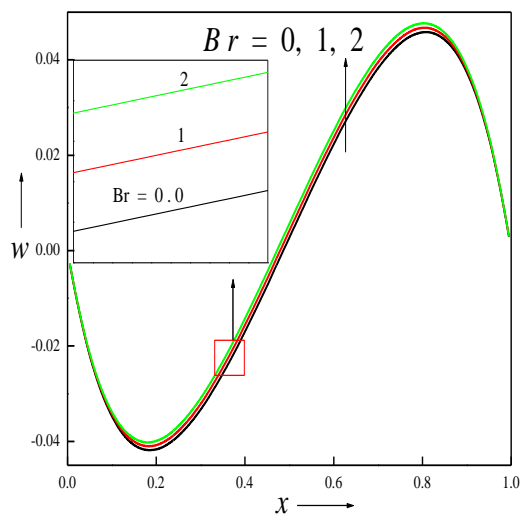(4a)

(4b)   (4c)

Figure 4. Velocity (4a, b) and temperature (4c) contours and profiles for different I
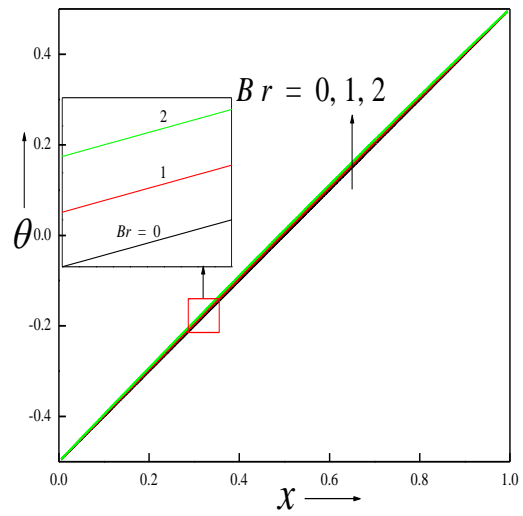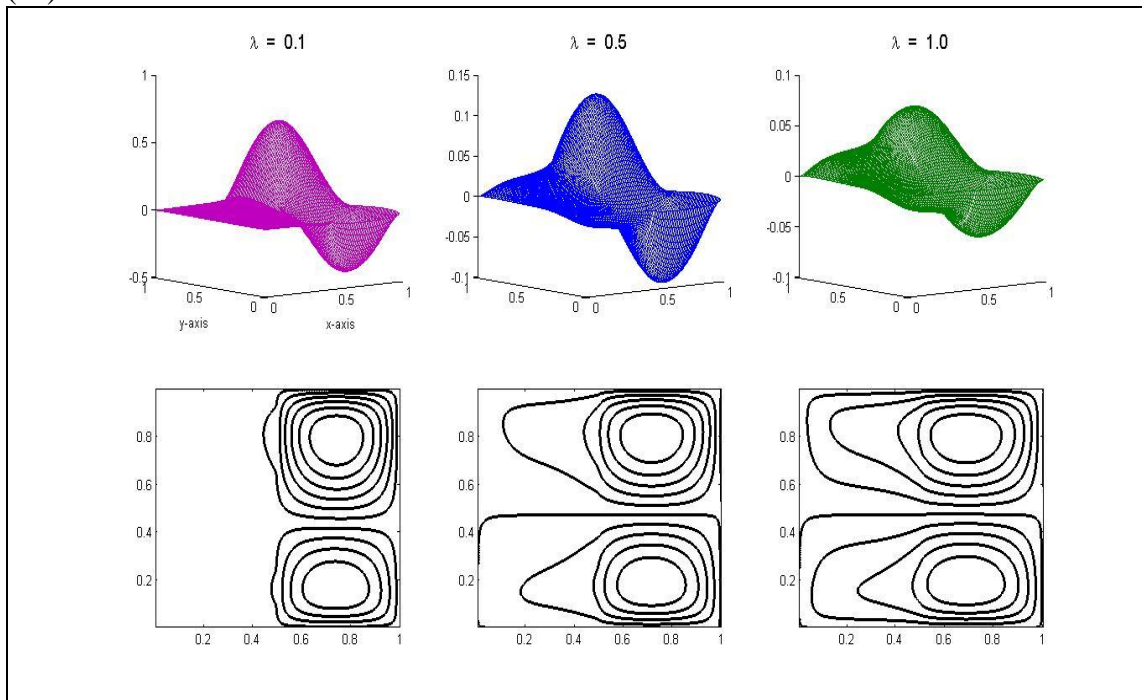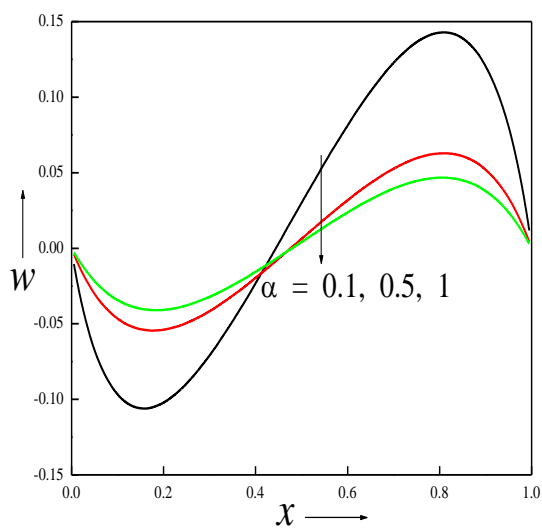
(5a)

(5b)

(5c)

Figure 5. Velocity (5a, b) and temperature (5c) contours and profiles for different *Br*
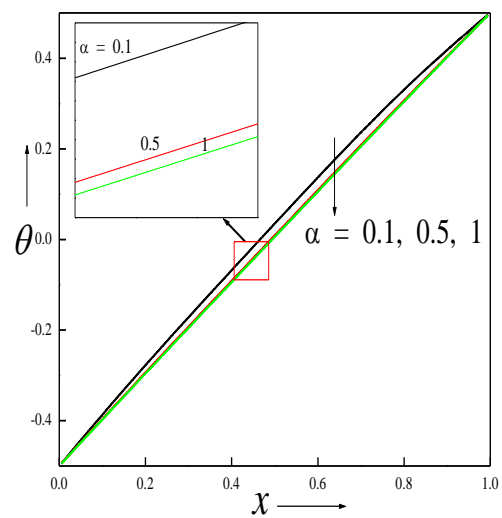
(6a)

(6b)

(6c)

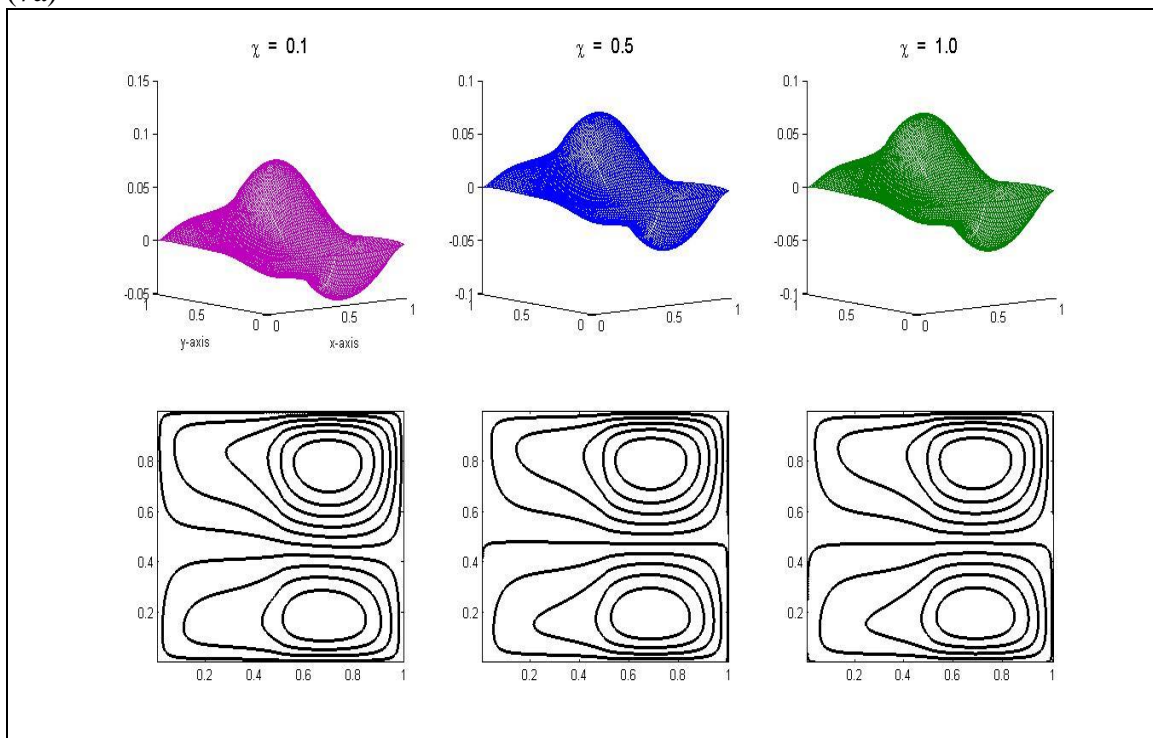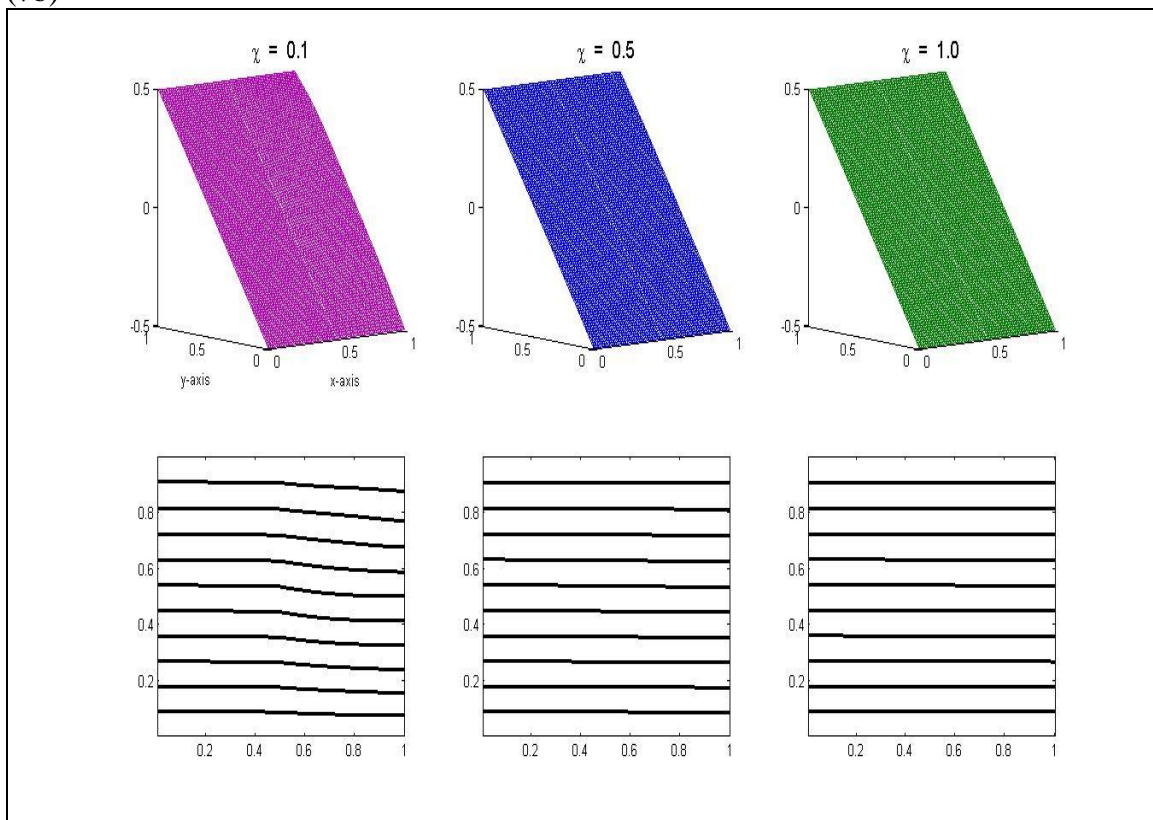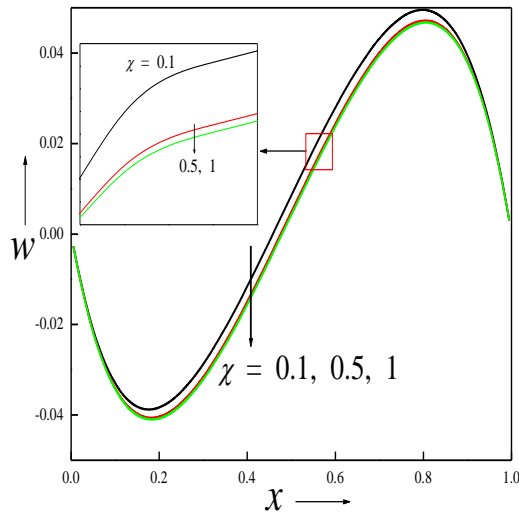**Figure 6.** Velocity (6a, b) and temperature (6c) contours and profiles for different α

(7a)

(7b)

(7c) (7d)
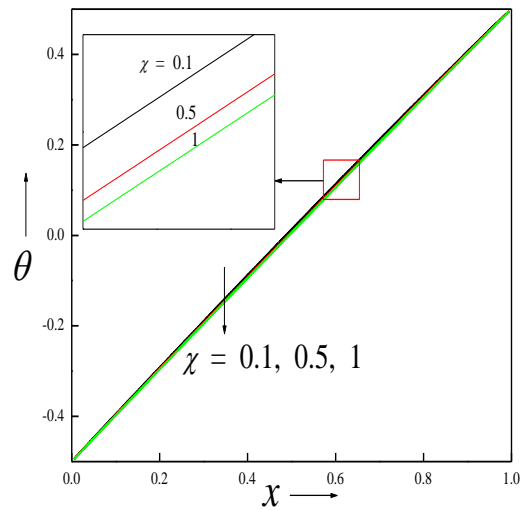
Figure 7. Velocity (7a, c) and temperature (7b, d) contours and profiles for different χ

Table 1. Grid independence test

Size of the grid	Region-1	Region-2
11×11	1.02405361854933	1.03226665365408
51×51	1.02377669154082	1.03360202945089
101×101	1.02378068569846	1.03364978587588
151×151	1.02378158702730	1.03365869051294
201×201	1.02378191542428	1.03366181226918

Table 2. Comparison for $Br = Ec = \text{Pr} = 1$, $P = -0.1$, $\lambda = 1$, $\beta = 1$, $\chi = 1$

	Present $(Da = 1, I = 4)$		Umavathi and Bég (2020) $(Da = 0, I = 0)$	
Gr	Region-1	Region-2	Region-1	Region-2
1	1.0003734744657	1.0003748511311	1.0003783577697	1.0003783577697
10	1.0435527851379	1.0439754132530	1.0444145000752	1.0444145000752
20	1.1656069078517	1.1676634911878	1.1699171414455	1.1699171414455

Table 3. Volumetric flow rate

		Volumetric Flow Rate	
		Region-1	Region-2
Gr			
0.0		0.000850282128275056	0.002184807922801564
1.0		0.000850639868417865	0.002186145002066430
10		0.001202846270591417	0.003243189801734679
Da			
0.000001		0.000000015729500906	0.001925163167817541
0.01		0.001202846270591417	0.003243189801734679
1.0		0.005661138851524346	0.005826400327368434
I			
0.0		0.001205630197327104	0.003245643130821721
4.0		0.001202846270591417	0.003243189801734679
8.0		0.001200081904799690	0.003240752368332471
Br			
0.0		0.000848684101737182	0.002183737570140714
1.0		0.001202846270591417	0.003243189801734679
2.0		0.001562484200892853	0.004319849760333960
λ			
0.1		0.003183676864360223	0.070585858124905310
0.5		0.001466473122143211	0.006736670074203001
1.0		0.001202846270591417	0.003243189801734679
χ			
0.1		0.001780004089626783	0.007766538485297454
0.5		0.001323353533740122	0.003870810823821523
1.0		0.001202846270591417	0.003243189801734679

Table 4. Skin friction

	Region-1		Region-2	
	$\left(\dfrac{dw}{dy}\right)_{y=0}$	$\left(\dfrac{dw}{dy}\right)_{y=1}$	$\left(\dfrac{dw}{dy}\right)_{y=0}$	$\left(\dfrac{dw}{dy}\right)_{y=1}$
Gr				
0.0	0.0098488530	-0.0098488530	0.0181377773	-0.0181377773
1.0	-0.0279502789	-0.0476509280	-0.0392296607	-0.0755190287
10	-0.3660944326	-0.3897374930	-0.5500956289	-0.5976449319
Da				
0.000001	-0.0000989799	-0.0001031051	-0.4630514858	-0.4957047084
0.01	-0.3660944326	-0.3897374930	-0.5500956289	-0.5976449319
1.0	-0.5960329782	-0.6678486590	-0.6012725456	-0.6749302692
I				

0.0	-0.3662633391	-0.3899487199	-0.5501492862	-0.5977280479
4.0	-0.3660944326	-0.3897374930	-0.5500956289	-0.5976449319
8.0	-0.3659261082	-0.3895271481	-0.5500421569	-0.5975621982
Br				
0.0	-0.3679967978	-0.3876673947	-0.5555390474	-0.5918004152
1.0	-0.3660944326	-0.3897374930	-0.5500956289	-0.5976449319
2.0	-0.3642119428	-0.3918830336	-0.5446850423	-0.6036978433
λ				
0.1	-0.3917853506	-0.4372797012	-4.469308047	-5.3596613930
0.5	-0.3803449323	-0.4071583198	-1.021760996	-1.1191915300
1.0	-0.3660944326	-0.3897374930	-0.550095628	-0.5976449319
χ				
0.1	-0.3633573809	-0.3929958459	-0.5279281903	-0.6259044060
0.5	-0.3654998540	-0.3903961688	-0.5468683154	-0.6012845736
1.0	-0.3660944326	-0.3897374930	-0.5500956289	-0.5976449319

Table 5. Average Nusselt number

	Region-1		Region-2	
	$\left(\dfrac{dT}{dy}\right)_{y=0}$	$\left(\dfrac{dT}{dy}\right)_{y=1}$	$\left(\dfrac{dT}{dy}\right)_{y=0}$	$\left(\dfrac{dT}{dy}\right)_{y=1}$
Gr				
0.0	1.00006139831	0.999938601684	1.000090226778	0.999909773220
1.0	1.00020501063	0.999580032220	1.000265040552	0.999363953084
10	1.02378068569	0.973330685655	1.033649785875	0.961175369387
Da				
0.000001	1.00614730373	0.993395593238	1.022956882284	0.973883029103
0.01	1.02378068569	0.973330685655	1.033649785875	0.961175369387
1.0	1.04355278513	0.947957792504	1.043975413253	0.947309812445
I				
0.0	1.02381274424	0.973289716789	1.033667135415	0.961152678748
4.0	1.02378068569	0.973330685655	1.033649785875	0.961175369387
8.0	1.02374878867	0.973371421240	1.033632524537	0.961197932366
Br				
0.0	0.99999999993	1.00000000006	0.999999999936	1.000000000062
1.0	1.023780685698	0.973330685655	1.033649785875	0.961175369387
2.0	1.04707791512	0.945628144311	1.066231455491	0.920425543160
λ				
0.1	1.08311476452	0.895223522022	1.222284258805	0.673008140285
0.5	1.03171033782	0.964043438812	1.056842244289	0.932726223093
1.0	1.02378068569	0.973330685655	1.033649785875	0.961175369387
χ				
0.1	1.03381369068	0.960144280765	1.216410180045	0.683065608990

| 0.5 | 1.02784478571 | 0.968592747828 | 1.058360368768 | 0.930316538235 |
| 1.0 | 1.02378068569 | 0.973330685655 | 1.033649785875 | 0.961175369387 |

Conflict of interest: The authors do not have any conflict of interest

References

Alzami, B. and Vafai, K. (2001), "Analysis of fluid flow and heat transfer interfacial conditions between a porous medium and a fluid layer", Int. J. Heat and Mass Transfer, Vol. 44, pp. 1735-1749.

Amiri, A. and Vafai, K. (1995), "Effects of boundary conditions on non-Darcian heat transfer through porous media and experimental comparisons", Num Heat Transfer, Vol. 27, pp. 651-664.

Amiri, A. and Vafai, K. (1994), "Analysis of dispersion effects and non-thermal equilibrium, non-Darcian, variable-porosity incompressible flow through porous Media", Int. J. Heat Mass Transfer, Vol. 37, pp. 939-954.

Arquis, E. and Caltagirone, J.P. (1987), "Interacting convection between fluid and open porous layers", ASME paper No. 87-WA/HT-24.

Arzhang, K., Shivakumara, I.S. and Suma, S.P., (2003), "Convective instability in superposed fluid and porous layers with vertical through flow", Transport in Porous Media, Vol. 51, pp. 1–18.

Bagchi, A. and Kulacki, F.A., (2020), "Natural convection in superposed fluid-porous layers", Springer Briefs in Thermal Engineering and Applied Science, Springer Nature.

Baytas, A.C. and Pop, I. (1999), "Free convection in oblique enclosures filled with a porous medium", Int. J. Heat Mass Transfer, Vol. 42, pp. 1047–1057.

Beckermann, C., Viskanta, R. and Ramadhyani, S. (1987), "Natural convection flow and heat transfer between a fluid layer and a porous layer inside a

rectangular enclosure, ASME J. Heat Transfer, Vol. 109, pp. 363-370.

Beckermann, C., Viskanta, R. and Ramadhyani, S. (1986), "A numerical study of non-Darcian natural convection in a vertical enclosure filled with a porous medium", Numer. Heat Transfer, Vol.**10**, pp. 557-570.

Bevers, G. and Joseph, D.D. (1967), "Boundary conditions at a naturally permeable wall", J. Fluid Mech., Vol. 30, pp. 197-207.

Borrelli, A., Giantesio, G. and Patria, M.C. (2017), " Reverse flow in magnetoconvection of two immiscible fluids in a vertical channel", ASME J. Fluids Eng., Vol. 139, pp. 101203 (16 pages).

Campos, H., Morales, J.C., Lacoa, U. and Campo, A. (1990), "Thermal aspects of a vertical annular enclosure divided into a fluid region and a porous region, Int. Comm. Heat Mass Transfer, Vol. 17**,** pp. 343-354.

Chikh, S., Boumedian, A., Bouhadef, K. and Lauriat, G. (1995), "Analytical solution of non-Darcian forced convection in an annular duct partially filled with porous medium, Int. J. Heat Mass Transfer, Vol. 38, pp. 1543-1551.

Christian, G. and Fryer, P. (2006), "The effect of pulsing cleaning chemicals on the cleaning of whey protein deposits", Food Bioprod. Process., Vol. 84, pp. 320–328.

Cole, P., Asteriadou, K., Robbins, P., Owen, E., Montague, G. and Fryer, P. (2010), "Comparison of cleaning of toothpaste from surfaces and pilot scale pipe work", Food Bioprod. Process., Vol. 88, pp. 392–400.

De Vahl Davis, G. (1968), "Laminar natural convection in an enclosed rectangular cavity" , Int. J. Heat Mass Transfer, Vol. 11, pp.167–1693.

De Vahl Davis, G. (1983), "Natural convection of air in a square cavity", Int. J. Num. Meth. Fluids, Vol. 3, pp. 249-264.

Du, Z.G. and Bilen, E. (1990), "Natural convection in vertical cavities with partially filled heat-generating porous medium", Numerical Heat Transfer, Vol. 18A, pp. 371-386.

Howell, P., Waters, S. and Grotberg, J. (2000), "The propagation of a liquid bolus along a liquid-lined flexible tube", J. Fluid Mech., Vol. 406, pp. 309–335.

Hulin, J., Znaien, J., Mendonca, L., Sourbier, A., Moisy, F., Salin, D. and Hinch, E.,

(2008), "Buoyancy driven interpenetration of immiscible fluids of different densities in a tilted tube", in APS Division of Fluid Dynamics (American Physical Society), Vol. 1.

Jaluria, Y. and Gebhart, B. (1988), *Buoyancy-induced Flows and Transport*, Hemisphere, Washington, USA.

Jones, M. C. and Persichetti, J. M. (1986), "Convective instability in packed beds", AIChemE J., Vol. 32, pp. 1555–1557.

Kapur, J.N. and Shukla, J.B. (1964), "The flow of incompressible immiscible fluids between two plates", Appl. Sci. Res., Vol. 13, pp. 55-60.

Kaviany, K. (1991), *Principles of Heat transfer in Porous Media,* Springer-Verlag, New York.

Kaviany, M. (1985), "Laminar flow through a porous channel bounded by isothermal parallel plates", Int. J. Heat Mass Transfer, Vol. 28**,** pp. 851-858.

Kim, S.J. and Choi, C.Y. (1996), "Convection heat transfer in porous and overlying layers heated from below", Int. J. Heat Mass Transfer, Vol. 39, pp. 319-329.

Kim, S.Y., Kang, B.H. and Hyuan, J. M. (1994), "Heat transfer from pulsating flow in a Channel filled with porous media", Int. J. Heat Mass Transfer, Vol. 37, pp. 2025-2033.

Kuznetsov, A.V., (1999), "A boundary layer solution for the momentum and energy transport in the interface region between a porous medium and a fluid layer", 33rd National Heat Transfer Conference NHTC'99, Albuquerque, NM (USA), 08/15/1999--08/17/1999.

Lewis, R.W. and Nithiarasu, P. and Seetharamu, K.N., (2004), *Fundamentals of the Finite Element Method for Heat and Fluid Flow,* John Wiley and Sons, New York, USA.

Lewis, R.W. and Schrefler, B.A. (1998), *The Finite Element Method In The Static and Dynamic Deformation and Consolidation of Porous Media,* John Wiley and Sons, New York, USA.

Liu, I.C., Umavathi, J.C. and Wang, H.H. (2012), "Poiseuille-Couette flow and heat transfer in an inclined composite porous medium", J. of Mechanics., Vol. 28, pp. 559-566.

Malashetty, M.S., Umavathi, J.C. and Prathap Kumar, J. (2004), "Two fluid flow and

heat transfer in an inclined channel containing porous and fluid layer, Heat and Mass Transfer, Vol. 40, pp. 871-876.

Malashetty, M.S., Umavathi, J.C. and Prathap Kumar, J. (2005), "Flow and heat transfer in an inclined channel containing a fluid layer sandwiched between two porous layers", Journal of Porous Media, Vol. 8, pp. 443-453.

Malashetty, M.S., Umavathi, J.C. and Prathap Kumar, J.: 2001, Convective flow and heat transfer in a composite porous medium, *Journal of Porous Media*, **4**, 15-22.

Manole, D.M. and Lage, J.L. (1992), "Numerical benchmark results for natural convection in a porous medium cavity", HTD, Heat and Mass Transfer in Porous Media, ASME Conference, Vol. 216, pp. 55-60.

Manu, C., Sabino, S., Iman, A., Mark, J.M., Chris, R.K. and Sasa, K. (2020), "Effect of packing height and location of porous media on heat transfer in a cubical cavity: Are extended Darcy simulations sufficient?", Int. J. Heat and Fluid Flow, Vol. 84, pp. 108617 (12 pages).

Min, J.Y. and Kim, S.J., (2005), "A novel methodology for thermal analysis of a composite system consisting of a porous medium and an adjacent fluid layer", ASME J. Heat Transfer, Vol. 127, pp. 648-656.

Mohamad, C. , Yousef, H and Bernd, M. (2020), "Upscaling LBM-TPM simulation approach of Darcy and non-Darcy fluid flow in deformable, heterogeneous porous media", *Int. J. Heat and Fluid Flow*, Vol. 83, pp. 108566 (13 pages).

Moshkin, N.P. (2002), "Numerical model to study natural convection in a rectangular enclosure filled with two immiscible fluids", Int. J. Heat and Fluid Flow, Vol. 23, pp. 373-379.

Neale, G. and Nader, W. (1974), "Practical significance of Brinkman's extension of Darcy's law: coupled parallel flows within a channel and a bounding porous Medium" , Can. J. Chem. Engng., Vol. 52, pp. 475-478.

Nield, D.A. and Bejan, A. (1999), *Convection in Porous Media*, Second ed., Springer-Verlag, New York.

Nithiarasu, P., Lewis, R.W. and Seetharamu, K.N. (2015), *Fundamentals of the Finite Element Method for Heat and Mass Transfer,* Second Edition, Wiley.

Oztop, H.F., Yasin Varol, Ahmet Koca, (2009), "Natural convection in a vertically

divided square enclosure by a solid partition into air and water regions", Int. J. Heat and Mass Transfer, Vol. 52, pp. 5909-5921.

Pop, I. and Ingham, D.B., (2001), *Convective Heat Transfer: Mathematical and Computational Modeling of Viscous Fluids and Porous Media*, Elsevier Science & Technology Books, The Netherlands.

Prasad, V. (1990), "Convection flow interaction and heat transfer between fluid and porous layers", Proc. NATO Advanced Study Institute on Convective Heat and Mass Transfer in Porous Media, Turkey.

Prasad, V. and Kulacki, F.A. (1984), "Convective heat transfer in a rectangular porous cavity-effect of aspect ratio on flow structure and heat transfer", ASME J. Heat Transfer, Vol. 106, pp. 158-165.

Redapangu, P., Vanka, S. and Sahu, K. (2012), "Multiphase lattice Boltzmann simulations of buoyancy-induced flow of two immiscible fluids with different viscosities", Eur. J. Mech.-B Fluids, Vol. 34, pp. 105–114.

Regner, M., Henningsson, M., Wiklund, J., O¨ stergren, K. and Tragardh, C. (2007), "Predicting the displacement of yoghurt by water in a pipe using CFD", Chem. Eng. Technol., Vol. 30, pp. 844–853.

Sahu, K. and Vanka, S. (2011), "A multiphase lattice Boltzmann study of buoyancy induced mixing in a tilted channel", Comput. Fluids, Vol. 50, pp. 199–215.

Shail, R. (1973), "On laminar two-phase flow in magneto hydrodynamics", Int. J. Eng. Sci., Vol. 11, pp. 1103–1108.

Song, M. and Viskanta, R. (1994), "Natural convection flow and heat transfer within a rectangular enclosure containing a vertical porous layer", Int. J. Heat MassTransfer, Vol. 37, pp. 2425-2438.

Sozen, M. and Kuzay, T.M. (1996), "Enhanced heat transfer in round tubes with porous inserts", Int. J. Heat Fluid Flow, Vol. 17, pp. 124-129.

Srinivas, J. and Ramana Murthy, J.V. (2016a), "Flow of two immiscible couple stress fluids between two permeable beds", J. Appl. Fluid Mech., Vol. 9, pp. 501-507.

Srinivas, J. and Ramana Murthy, J.V., (2016b), "Second law analysis of the flow of two immiscible micropolar fluids between two porous beds*", J. Eng. Thermophys*, Vol. 25, pp. 126 -142.

Srinivasan, V. and Vafai, K. (1994), "Analysis of linear encroachment in two immiscible fluid systems in a porous medium", ASME J. Fluids Eng., Vol. 116, pp. 135-139.

Tien, C.L. and Vafai, K. (1989), "Convective and radiative heat transfer in porous media", Advances in Appl. Mech., Vol. 27, pp. 225-281.

Umavathi, J.C. and Bég, O.A., (2020), "Effects of thermo physical properties on heat transfer at the interface of two immiscible fluids in a vertical duct: Numerical study", Int. J. of Heat and Mass Transfer, Vol. 154, pp.119613 (18 pages)

Umavathi, J.C. and Santosh, V. (2012a), "Non-Darcy mixed convection in a vertical porous channel with boundary conditions of third kind", Trans. Porous Media, Vol. 95, pp. 111-131.

Umavathi, J.C. and Shekar, M. (2014), "Mixed convective flow of immiscible fluids in a vertical corrugated channel with traveling thermal waves", J. King Saud University- Engineering Sciences, Vol. 26, pp. 49-68.

Umavathi, J.C. and Sheremet, M. (2019), "Flow and heat transfer of couple stress nanofluid sandwiched between viscous fluids", *Int. J. Numerical Methods for Heat and Fluid Flow,* Vol. 29, pp. 4262-4276.

Umavathi, J.C., (2013), "Analysis of flow and heat transfer in a vertical rectangular duct using a non-Darcy model", Trans. Porous Media, Vol. 96, pp. 527–545.

Umavathi, J.C., (2015a), "Free convective flow in a vertical rectangular duct filled with porous matrix for viscosity and conductivity variable properties", Int. J. Heat and Mass Transfer, Vol. 81, 383-403.

Umavathi, J.C., (2015b), "Combined effect of variable viscosity and variable thermal conductivity on double diffusive convection flow of a permeable fluid in a vertical channel", Trans. Porous Media, Vol. 108, pp. 659-678.

Umavathi, J.C., Chamkha, A.J. and Sridhar, K.S.R., (2010), "Generalised plain Couette flow heat transfer in a composite channel, Trans. Porous Media, Vol. 85, pp. 157-169.

Umavathi, J.C., Chamkha, A.J., Mateen, A. and Al-Mudhaf, A. (2005), "Unsteady two fluid flow and heat transfer in a horizontal channel", Heat Mass Transfer, Vol. 42, pp. 81-90.

Umavathi, J.C., Malashetty, M.S. and Mateen, A. (2004), "Fully developed flow and heat

transfer in a horizontal channel containing an electrically conducting fluid sandwiched between two fluid layers", Int. J. Applied Mechanics and Eng., Vol. 9, pp. 781-794.

Umavathi, J.C., Prathap Kumar, J. and Jaweriya, S. (2012b), "Mixed convection flow in a vertical porous channel with boundary conditions of third kind with heat source/sink", J. Porous Media, Vol. 15, pp. 998-1007.

Umavathi, J.C., Shaik Meera, D. and Liu, I.C., (2008), "Unsteady flow and heat transfer of three immiscible fluids", Int. J. Appl. Mech. Engg., Vol. 13, pp. 1079-1100.

Vafai, K. (2000), *Handbook of Porous Media*, Marcel Dekker, New York.

Vafai, K. and Kim, S. (1989), "Forced convection in a channel filled with porous medium: and exact solution", ASME J. Heat Transfer, Vol. 111, pp. 1103-1106.

Vafai, K. and Kim, S.J. (1990), "Fluid mechanics of the interface region between a porous medium and a fluid layer-an exact solution", Int. J. Heat Fluid Flow, Vol. 11, pp. 254-256.

Vafai, K. and Thiyagaraja, R. (1987), "Analysis of flow and heat transfer at the interface region of a porous medium", Int. J. Heat Mass Transfer, Vol. 30, pp. 1391-1405.

Valette, R., Laure, P., Demay, Y. and Agassant, J. (2004), "Convective linear stability analysis of two-layer co extrusion flow for molten polymers, J. Non-Newtonian Fluid Mech., Vol. 121, pp. 41–53.